

1 **REVISION 1**

2
3 **Vanadio-oxy-chromium-dravite, $\text{NaV}_3(\text{Cr}_4\text{Mg}_2)(\text{Si}_6\text{O}_{18})(\text{BO}_3)_3(\text{OH})_3\text{O}$, a new**
4 **mineral species of the tourmaline supergroup**

5
6 FERDINANDO BOSI¹, LEONID REZNITSKII², HENRIK SKOGBY³ AND ULF HÅLENIUS³

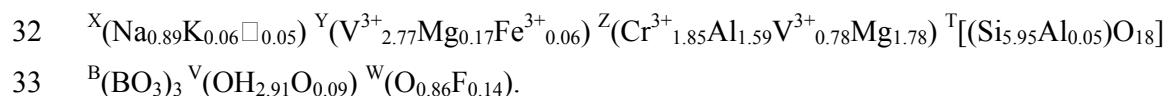
7
8 ¹Dipartimento di Scienze della Terra, Sapienza Università di Roma, P.le A. Moro, 5, I-00185 Rome,
9 Italy

10 ²Russian Academy of Science. Siberian Branch, Institute of the Earth's crust, Lermontova str., 128,
11 Irkutsk, Russia

12 ³Department of Geosciences, Swedish Museum of Natural History, Box 50007, SE-10405 Stockholm,
13 Sweden

14
15
16
17 **ABSTRACT**

18 Vanadio-oxy-chromium-dravite, $\text{NaV}_3(\text{Cr}_4\text{Mg}_2)(\text{Si}_6\text{O}_{18})(\text{BO}_3)_3(\text{OH})_3\text{O}$, is a new
19 mineral of the tourmaline supergroup. It is found in metaquartzites of the Pereval marble
20 quarry (Sludyanka, Lake Baikal, Russia) in association with quartz, Cr-V-bearing tremolite
21 and muscovite–celadonite–chromphyllite–roscoelite, diopside–kosmochlor–natalyite, Cr-
22 bearing goldmanite, escolaitite–karelianite, dravite–oxy-vanadium-dravite, V-bearing titanite
23 and rutile, ilmenite, oxyvanite–berdesinskiite, shreyerite, plagioclase, scapolite, zircon, pyrite
24 and an unnamed oxide of V, Cr, Ti, U and Nb. Crystals are emerald green, transparent with a
25 vitreous luster, pale green streak and conchoidal fracture. Vanadio-oxy-chromium-dravite has
26 a Mohs hardness of approximately $7\frac{1}{2}$, and a calculated density of 3.3 g/cm^3 . In plane
27 polarized light, vanadio-oxy-chromium-dravite is pleochroic (O = dark green, E = pale green)
28 and uniaxial negative: $\omega = 1.767(5)$, $\varepsilon = 1.710(5)$. Vanadio-oxy-chromium-dravite is
29 rhombohedral, space group $R3m$, with the unit-cell parameters $a = 16.1260(2)$, $c = 7.3759(1)$
30 Å, $V = 1661.11(4) \text{ Å}^3$, $Z = 3$. Crystal chemistry analysis resulted in the empirical structural
31 formula:



34 The crystal structure of vanadio-oxy-chromium-dravite was refined to a statistical
35 index *R*1 of 1.16% using 2543 unique reflections collected with MoK α X-radiation. Ideally,
36 vanadio-oxy-chromium-dravite is related to oxy-chromium-dravite and oxy-vanadium-dravite
37 by the homovalent substitution $\text{V}^{3+} \leftrightarrow \text{Cr}^{3+}$. Tourmaline with chemical compositions classified
38 as vanadio-oxy-chromium-dravite can be either Cr^{3+} -dominant or V^{3+} -dominant as a result of
39 the compositional boundaries along the solid solution between Cr^{3+} and V^{3+} that are
40 determined at $^{Y+Z}(\text{V}_5\text{Cr}_2)$, corresponding to $\text{Na}^Y(\text{V}_3)^Z(\text{V}_2\text{Cr}_2\text{Mg}_2)\text{Si}_6\text{O}_{18}(\text{BO}_3)_3(\text{OH})_3\text{O}$, and
41 $^{Y+Z}(\text{V}_{1.5}\text{Cr}_{5.5})$, corresponding to $\text{Na}^Y(\text{V}_{1.5}\text{Cr}_{1.5})^Z(\text{Cr}_4\text{Mg}_2)\text{Si}_6\text{O}_{18}(\text{BO}_3)_3(\text{OH})_3\text{O}$.

42

43

44

INTRODUCTION

45 The tourmaline supergroup minerals are widespread, occurring in sedimentary, igneous
46 and metamorphic settings. They are important indicator minerals that can provide information
47 on the compositional evolution of their host rocks, chiefly due to their ability to incorporate a
48 large number of elements (e.g., Novák et al. 2004; Agrosi et al. 2006; Lussier et al. 2011a;
49 Novák et al. 2011; van Hinsberg et al. 2011; Bačík et al. 2012). However, the chemical
50 composition of tourmalines is also controlled by short-range and long-range constraints (e.g.,
51 Hawthorne 1996, 2002; Bosi and Lucchesi 2007; Bosi 2010, 2011; Henry and Dutrow 2011;
52 Skogby et al. 2012; Bosi 2013) as well as by temperature (van Hinsberg and Schumacher
53 2011). Tourmaline supergroup minerals are complex borosilicates and their crystal structure
54 and crystal chemistry have been extensively studied (e.g., Foit 1989; Hawthorne and Henry
55 1999; Bosi and Lucchesi 2007; Lussier et al. 2008; Bosi 2008; Bosi et al. 2010; Lussier et al.
56 2011b; Filip et al. 2012). In accordance with Henry et al. (2011), the general formula of
57 tourmaline may be written as: $\text{XY}_3\text{Z}_6\text{T}_6\text{O}_{18}(\text{BO}_3)_3\text{V}_3\text{W}$, where $\text{X} (\equiv [^9]\text{X}) = \text{Na}^+, \text{K}^+, \text{Ca}^{2+}, \square$
58 (\equiv vacancy); $\text{Y} (\equiv [^6]\text{Y}) = \text{Al}^{3+}, \text{Fe}^{3+}, \text{Cr}^{3+}, \text{V}^{3+}, \text{Mg}^{2+}, \text{Fe}^{2+}, \text{Mn}^{2+}, \text{Li}^+$; $\text{Z} (\equiv [^6]\text{Z}) = \text{Al}^{3+}, \text{Fe}^{3+},$
59 $\text{Cr}^{3+}, \text{V}^{3+}, \text{Mg}^{2+}, \text{Fe}^{2+}$; $\text{T} (\equiv [^4]\text{T}) = \text{Si}^{4+}, \text{Al}^{3+}, \text{B}^{3+}$; $\text{B} (\equiv [^3]\text{B}) = \text{B}^{3+}$; $\text{W} (\equiv [^3]\text{O1}) = \text{OH}^{1-}, \text{F}^{1-},$
60 O^{2-} ; $\text{V} (\equiv [^3]\text{O3}) = \text{OH}^{1-}, \text{O}^{2-}$ and where, for example, T represents a group of cations ($\text{Si}^{4+},$
61 $\text{Al}^{3+}, \text{B}^{3+}$) accommodated at the [4]-coordinated T sites. The dominance of these ions at one or
62 more sites of the structure gives rise to a range of distinct mineral species.

63 Recently, several new minerals of the tourmaline supergroup were approved by the
64 Commission on New Minerals, Nomenclature and Classification (CNMNC) of the

65 International Mineralogical Association (IMA). Among these are a number of oxy-tourmalines
66 related by the complete solid solution in the Al^{3+} - Cr^{3+} - V^{3+} subsystem: oxy-dravite, end-
67 member formula $NaAl_3(Al_4Mg_2)(Si_6O_{18})(BO_3)_3(OH)_3O$ (IMA 2012-004a; Bosi and Skogby
68 2013), oxy-chromium-dravite, $NaCr_3(Cr_4Mg_2)(Si_6O_{18})(BO_3)_3(OH)_3O$ (IMA 2011-097; Bosi et
69 al. 2012a); oxy-vanadium-dravite, $NaV_3(V_4Mg_2)(Si_6O_{18})(BO_3)_3(OH)_3O$ (IMA 11-E; Bosi et al.
70 2013a).

71 A new species of oxy-tourmaline, vanadio-oxy-chromium-dravite, has been approved
72 by the Commission on New Minerals, Nomenclature and Classification of the International
73 Mineralogical Association (IMA 2012-034). The holotype specimen (sample PR76) is
74 deposited in the collections of the Museum of Mineralogy, Earth Sciences Department,
75 Sapienza University of Rome, Italy, catalogue number 33067. A formal description of the new
76 species vanadio-oxy-chromium-dravite (V^{3+} -rich tourmaline) is presented here, including a
77 full characterization of its physical, chemical and structural properties. After the sample PR76
78 ($Cr_2O_3 = 12.9$ wt%) was approved as a new mineral species by the CNMNC-IMA, another
79 sample (PR1973) showing higher contents of Cr_2O_3 (24.5 wt%) was found from the same
80 locality. The composition of latter sample is closer to the vanadio-oxy-chromium-dravite end-
81 member. Consequently, we will here present chemical and structural data for both of these
82 samples.

83

84

85 OCCURRENCE, APPEARANCE AND PHYSICAL AND OPTICAL PROPERTIES

86 The crystals of vanadio-oxy-chromium-dravite occur in metaquartzites in the Pereval
87 marble quarry, Sludyanka crystalline complex, Southern Baikal region, Russia ($51^{\circ}37'N$
88 $103^{\circ}38'E$). The Pereval quarry is the type locality (see Bosi et al. 2012a for a more detailed
89 description) for natalyite, florensovite, kalininite, magnesiocoulsonite, oxy-vanadium-dravite,
90 batisivite, oxyvanite and cuprokalininite. Minerals associated with the holotype specimen
91 PR76 are: quartz, Cr-V-bearing tremolite and dioctahedral mica (muscovite–celadonite–
92 chromphyllite–roscoelite), diopside–kosmochlor–natalyite, Cr-bearing goldmanite, escolaitite–
93 karelianite, dravite–oxy-vanadium-dravite, V-bearing titanite and rutile, ilmenite, oxyvanite–
94 berdesinskiite, shreyerite, plagioclase, scapolite, zircon, pyrite and an unnamed oxide of V, Cr,
95 Ti, U and Nb, whereas minerals associated with sample PR1973 are: quartz, calcite, Cr-V-
96 bearing diopside and tremolite, V-bearing magnesiochromite, goldmanite–uvarovite,

97 karelianite–escolaite and V-Cr tourmalines. The host rocks (quartz–diopside) are Cr-V-bearing
98 carbonate-siliceous sediments, metamorphosed to granulite facies and partly diaphthorized to
99 amphibolite facies (retrograde stage). Vanadio-oxy-chromium-dravite was formed in the
100 prograde stage (granulite facies). The crystals are euhedral, reaching up to 0.3 mm in length,
101 and may be chemically zoned, but homogeneous crystals also occur.

102 The vanadio-oxy-chromium-dravite morphology consists of elongated $\{10\bar{1}0\}$ and
103 $\{11\bar{2}0\}$ prisms terminated by a prominent $\{0001\}$ pation and small, minor $\{10\bar{1}1\}$ pyramidal
104 faces. Crystals are emerald green, with pale green streak, transparent and display vitreous
105 luster. They are brittle and show conchoidal fracture. The Mohs hardness is approximately $7\frac{1}{2}$
106 (Reznitsky et al. 2001). The calculated density is 3.279 g/cm^3 and 3.313 g/cm^3 for samples
107 PR76 and PR1973, respectively. In transmitted light, vanadio-oxy-chromium-dravite is
108 pleochroic with O = dark green and E = pale green. Vanadio-oxy-chromium-dravite is uniaxial
109 negative with refractive indices, measured by the immersion method using white light from a
110 tungsten source, of $\omega = 1.767(5)$, $\epsilon = 1.710(5)$ (sample PR76).

111

112

113

METHODS

114 Single-crystal structural refinement

115 As mentioned previously, two crystals of the mineral (from holotype sample PR76 and
116 specimen PR1973 which is closer to end-member composition) were selected for X-ray
117 diffraction measurements on a Bruker KAPPA APEX-II single-crystal diffractometer, at
118 Sapienza University of Rome (Earth Sciences Department), equipped with a CCD area
119 detector ($6.2 \times 6.2 \text{ cm}^2$ active detection area, 512×512 pixels) and a graphite crystal
120 monochromator, using $\text{MoK}\alpha$ radiation from a fine-focus sealed X-ray tube. The sample-to-
121 detector distance was 4 cm. A total of ca. 2500-3500 exposures (step = 0.2° , time/step = 20 s)
122 covering a full reciprocal sphere with a redundancy of about 8 was used. Final unit-cell
123 parameters were refined by means of the Bruker AXS SAINT program using reflections with I
124 $> 10 \sigma(I)$ in the range $5^\circ < 2\theta < 78^\circ$. The intensity data were processed and corrected for
125 Lorentz, polarization, and background effects with the APEX2 software program of Bruker
126 AXS. The data were corrected for absorption using the multi-scan method (SADABS). The
127 absorption correction led to a significant improvement in R_{int} . No violations of $R3m$ symmetry
128 were noted.

129 Structural refinement was done with the SHELXL-97 program (Sheldrick 2008).
130 Starting coordinates were taken from Bosi et al. (2004). Variable parameters were: scale
131 factor, extinction coefficient, atomic coordinates, site scattering values and atomic
132 displacement factors. To obtain the best values of statistical indexes ($R1$, $wR2$), a fully ionized
133 scattering curve for O was used, whereas neutral scattering curves were used for the other
134 atoms. In detail, the X and Y site were modeled by using Na and V scattering factors
135 (respectively), while the occupancy of the Z site was modeled considering the presence of Cr
136 and Mg. The T and B sites were modeled, respectively, with Si and B scattering factors and
137 with a fixed occupancy of 1, because refinement with unconstrained occupancies showed no
138 significant deviations from this value. Three full-matrix refinement cycles with isotropic
139 displacement parameters for all atoms were followed by anisotropic cycles until convergence
140 was attained. No significant correlations over a value of 0.7 between the parameters were
141 observed at the end of refinement. Table 1 lists crystal data, data collection information and
142 refinement details; Table 2 gives the fractional atomic coordinates and site occupancies; Table
143 3 gives the displacement parameters; Table 4 gives selected bond distances.

144

145 **X-ray powder diffraction**

146 The X-ray powder-diffraction pattern for a small quantity of the vanadio-oxy-
147 chromium-dravite sample (PR76) was collected using a Panalytical X'pert powder
148 diffractometer equipped with an X'celerator silicon-strip detector. The range 5-70° (2θ) was
149 scanned with a step-size of 0.017° during 4 hours using a sample spinner with the sample
150 mounted on a background-free holder. The diffraction data (in Å for $CuK\alpha$, $\lambda_{\alpha_1} = 1.54060$ Å),
151 corrected using Si as an internal standard, are listed in Table 5. Since very limited amounts of
152 sample material were available, only the stronger lines could be recorded.

153

154 **Electron microprobe analysis**

155 Electron microprobe analyses of the crystals used for X-ray diffraction refinements
156 were obtained by wavelength-dispersive spectroscopy with a Cameca SX50 instrument at the
157 “Istituto di Geologia Ambientale e Geoingegneria CNR” (Rome, Italy), operating at an
158 accelerating potential of 15 kV and a sample current of 15 nA, with a 10 μ m beam diameter.
159 Minerals and synthetic compounds were used as standards: wollastonite (Si, Ca), magnetite
160 (Fe), rutile (Ti), corundum (Al), vanadinite (V) fluorphlogopite (F), periclase (Mg), jadeite

161 (Na), K-feldspar (K), sphalerite (Zn), metallic Cr, Mn and Cu. The overlap corrections and the
162 PAP routine were applied. The results, which are summarized in Table 6, represent mean
163 values of 10 spot analyses. In accordance with the documented very low concentration of Li in
164 dravitic samples (e.g., Henry et al. 2011), the Li₂O content was assumed to be insignificant.
165 Manganese and Cu and were found to be below their respective detection limits (0.03 wt%) in
166 both studied samples.

167

168 **Infrared spectroscopy**

169 A homogeneous vanadio-oxy-chromium-dravite crystal (sample PR76) was measured
170 by Fourier transform infrared (FTIR) absorption spectroscopy in the wavenumber range 2000-
171 5000 cm⁻¹ using a Bruker Equinox 55 spectrometer equipped with a NIR source, a CaF₂ beam-
172 splitter and an InSb detector. Polarized spectra with a resolution of 4 cm⁻¹ were obtained
173 parallel and perpendicular to the **c** axis using a wire-grid polarizer (KRS-5) and a circular
174 measurement area of 100 μm diameter on a 34 μm thick doubly-polished crystal plate that had
175 been oriented parallel the **c** axis by morphology and optical microscopy. Fundamental (OH)
176 absorption bands polarized parallel to the **c** axis direction of tourmalines may be exceptionally
177 intense, and as often observed, it was not possible to thin the sample sufficiently to avoid off-
178 scale absorption intensity for the strongest bands (Fig. 1). An unpolarized spectrum was
179 therefore obtained on a powdered crystal which confirmed that the main band does not consist
180 of multiple components.

181

182 **Optical absorption spectroscopy**

183 Polarized, room-temperature optical absorption spectra were recorded in the spectral
184 range 270-1100 nm (37037-9091 cm⁻¹) on a 25 μm thick, doubly-sided polished (100) platelet
185 of a tourmaline single crystal (sample PR76) at a spectral resolution of 1 nm using an
186 AVASPEC-ULS2048X16 spectrometer attached via a 400 μm UV optical fiber to a Zeiss
187 Axiotron UV-microscope. A 75 W Xenon arc lamp served as illuminating source and Zeiss
188 Ultrafluar 10x lenses served as objective and condenser. A UV-quality Glan-Thompson prism
189 with a working range from 250 to 2700 nm (40000 to 3704 cm⁻¹) was used as polarizer. The
190 size of the circular measure aperture was 64 μm in diameter. The wavelength scale of the
191 spectrometer was calibrated against Ho₂O₃-doped and Pr₂O₃/Nd₂O₃-doped standards (Hellma
192 glass filters 666F1 and 666F7) with an accuracy better than 15 cm⁻¹ in the wavelength range

193 300-1100 nm. Recorded spectra were fitted using the Jandel PeakFit 4.12 software assuming
194 Gaussian peak shapes.

195

196

197

RESULTS AND DISCUSSION

198 **General comment**

199 The present crystal structure refinements and electron microprobe analyses were
200 obtained from the same individual crystals from the two samples (PR76 and PR1973).
201 However, complementary powder X-ray diffraction data, FTIR spectra, optical absorption
202 spectra and refractive indices for sample PR76 were recorded from coexisting crystals. Small
203 differences in composition are likely to occur between these crystals.

204

205 **Determination of atomic proportions**

206 In agreement with the structural refinement results, the boron content was assumed to
207 be stoichiometric in both vanadio-oxy-chromium-dravite samples ($B = 3.00$ apfu). In fact, both
208 the site-scattering results and the bond lengths of B and T are consistent with the B site fully
209 occupied by boron and no amount of B at the T site. All iron was calculated as Fe^{3+} because
210 this seems to be the dominant valence of iron in Cr-rich tourmaline (Bosi et al. 2013b). Note
211 that due to the relatively low concentrations of Fe, uncertainty on its oxidation state has small
212 influence on the overall charge calculations. The (OH) content can then be calculated by
213 charge balance with the assumption $(T + Y + Z) = 15.00$. The atomic proportions were
214 calculated on this assumption (Table 5). The excellent match between the number of electrons
215 per formula unit (epfu) derived from chemical and structural analysis supports this procedure,
216 respectively: 281.4 epfu and 280.6 epfu for sample PR76; 288.0 and 287.7 for sample PR1973.

217

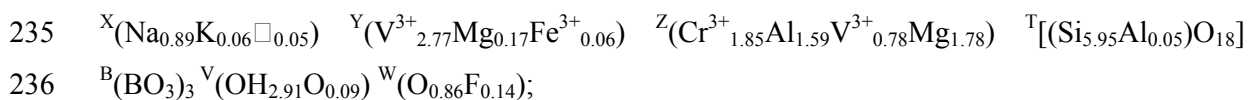
218 **Site populations**

219 The anion site populations in the studied samples follow the general preference
220 suggested for tourmaline (e.g., Grice and Ercit 1993; Henry et al. 2011): the O3 site (V
221 position in the general formula) is occupied by (OH) and O^{2-} , while the O1 site (W position in
222 the general formula) is occupied by O^{2-} and F. The cation distribution at the T , Y and Z sites
223 was optimized by using a least-squares program to minimize the residuals between calculated
224 and observed data (based on the chemical and structural analysis). Site-scattering values,
225 octahedral and tetrahedral mean bond-distances (i.e., $\langle Y-O \rangle$, $\langle Z-O \rangle$ and $\langle T-O \rangle$) were

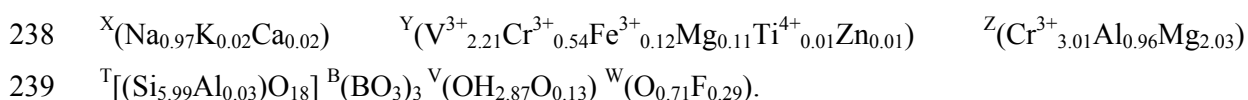
226 calculated as the linear contribution of each cation multiplied by its ideal bond-distance (Table
227 6). More details about the ideal distances as well as about the optimization procedure may be
228 found in Bosi et al. (2004) and Bosi and Lucchesi (2004; 2007). The robustness of this
229 approach was confirmed by another optimization procedure (Wright et al. 2000), which led to
230 very similar cation distributions (Table 6). This result represents another example of
231 convergence of these two procedures to similar solutions for tourmaline (e.g., Bosi and
232 Lucchesi 2007; Filip et al. 2012; Bosi et al. 2012a, 2013a).

233 The empirical structural formulae are as follows:

234 **sample PR76,**



237 **sample PR1973,**



240 The bond-valence analysis is consistent with the optimized structural formulae. Bond-valence
241 calculations, using the formula and bond-valence parameters from Brown and Altermatt
242 (1985), are reported in Table 7.

243

244 **Crystal chemistry**

245 The chemical composition of samples PR76 and PR1973 is consistent with tourmalines
246 belonging to the alkali group, oxy-subgroup 3 (Henry et al. 2011). They are Na-dominant at
247 the X site, oxygen-dominant at the W position, V^{3+} is the dominant cation at Y; Cr^{3+} is the
248 dominant cation at Z and Mg is the dominant divalent cation at Z. The end-member formula
249 may therefore be represented as $\text{NaV}_3(\text{Cr}_4\text{Mg}_2)\text{Si}_6\text{O}_{18}(\text{BO}_3)_3(\text{OH})_3\text{O}$. Because no tourmalines
250 have yet been documented as V^{3+} - and Cr^{3+} -dominant at Y and Z, respectively, this tourmaline
251 can be classified as a new species. Its closest end-member composition of a valid tourmaline
252 species is that of oxy-chromium-dravite (Bosi et al. 2012a), ideally
253 $\text{NaCr}_3(\text{Cr}_4\text{Mg}_2)\text{Si}_6\text{O}_{18}(\text{BO}_3)_3(\text{OH})_3\text{O}$. The name vanadio-oxy-chromium-dravite may hence be
254 assigned for the chemical composition, following Henry et al. (2011). The prefix *vandio*
255 represents the substitution, at the Y site, relative to the root composition of oxy-chromium-
256 dravite.

257 Although there exists a small degree of V^{3+} , Cr^{3+} and Mg disorder over Y and Z, the
258 structural formulae of samples PR76 and PR1973 indicate a clear preference of V^{3+} for the Y

259 site, while Cr^{3+} and Mg prefer the Z site. Aluminum is completely ordered at the Z site. The
260 O1 site population, characterized by O^{2-} with minor concentration of F, shows the absence of
261 (OH) contents. This finding is consistent with the observation of extremely weak absorption
262 bands occurring at wavenumbers higher than 3650 cm^{-1} in the infrared spectrum (Fig. 1),
263 typically ascribed to the O1 site (see below).

264

265 **Infrared spectroscopy**

266 Spectra recorded in polarized mode perpendicular and parallel to the crystallographic **c**
267 axis show an intense band around 3535 cm^{-1} and a very weak band at 3725 cm^{-1} , both
268 polarized in the **c** direction (Fig. 1). The main band around 3535 cm^{-1} can be related to the
269 local arrangement ($^{\text{Y}}\text{V}^{3+}\text{ }^{\text{Z}}\text{R}\text{ }^{\text{Z}}\text{R}$)-O3, i.e., to the occurrence of (OH) at the V position of the
270 tourmaline general formula (O3-site in the structure). Note that no significant absorption bands
271 occur at frequencies greater than 3650 cm^{-1} . This is consistent with the absence (or
272 insignificant concentrations) of (OH) at the W position (O1-site in the structure) (cf.
273 Gonzalez-Carreño et al. 1988; Bosi et al. 2012b; Bosi et al. 2013b).

274

275 **Optical absorption spectroscopy**

276 The polarized electronic spectra show two intense and broad absorption bands
277 observed at ~ 440 and 610 nm superimposed on an intense UV absorption (Fig. 2). Ligand
278 field theory predicts that energies of absorption bands caused by spin-allowed electronic *d-d*
279 transitions of octahedrally coordinated V^{3+} and Cr^{3+} should be comparable. The positions of
280 the two intense bands in the present spectra are indeed close to those of bands caused by spin-
281 allowed electronic *d-d* transitions in octahedrally coordinated Cr^{3+} in tourmaline (Taran et al.
282 1993; Ertl et al. 2008; Bosi et al. 2013b), but there exists a number of diagnostic differences.
283 The recorded bands occur at distinctly higher wavelengths than the spin-allowed absorption
284 bands caused by Cr^{3+} at the Z-site (425 and 574 nm ; Taran et al. 1993) or the Y-site (430 and
285 590 nm ; Bosi et al. 2013b) in tourmaline and, in addition to this, the diagnostic, narrow, spin-
286 forbidden Cr^{3+} -bands at $\sim 680\text{ nm}$ (Taran et al. 1993; Bosi et al. 2013b) are barely discernible
287 in the present spectra (Fig. 2). Comparable diagnostic differences were note in the spectra of a
288 set of V- and Cr-rich (OH)-bearing tourmaline samples (olenite and uvite) with variable V/Cr-
289 ratios by Ertl et al. (2008). Consequently, the broad and intense absorption bands at ~ 440 and
290 610 nm observed in the present spectra of vanadio-oxy-chromium-dravite are mainly caused
291 by spin-allowed *d-d* transitions in octahedrally coordinated V^{3+} . Contributions from absorption

292 at slightly lower wavelengths caused by octahedrally coordinated Cr^{3+} mainly result in
293 broadening of these V^{3+} -related absorption bands

294

295

296 COMPOSITIONAL BOUNDARIES OF VANADIO-OXY-CHROMIUM-DRAVITE

297

298 The plot of the Z- and Y-site cations in the ternary diagram for the Al-Cr- V^{3+}
299 subsystem show, of course, that vanadio-oxy-chromium-dravite is $^{\text{Z}}\text{Cr}$ -dominant and $^{\text{Y}}\text{V}$ -
300 dominant. More interesting, however, is the triangular plot in terms of Al-Cr- V^{3+} at Y and Z,
301 showing that vanadio-oxy-chromium-dravite can be either Cr^{3+} -dominant (sample PR1973) or
302 V^{3+} -dominant (sample PR76) (Fig. 3). This latter plot type displays the occurrence of three
303 end-members along the full solid solution between the Cr^{3+} and V^{3+} apices: oxy-chromium-
304 dravite, vanadio-oxy-chromium-dravite and oxy-vanadium-dravite. These end-members are
305 related by the substitution $\text{V}^{3+} \leftrightarrow \text{Cr}^{3+}$ at the Y position (vanadio-oxy-chromium-dravite \leftrightarrow
306 oxy-chromium-dravite) and $\text{V}^{3+} \leftrightarrow \text{Cr}^{3+}$ at the Z position (oxy-vanadium-dravite \leftrightarrow vanadio-
307 oxy-chromium-dravite), while their compositional boundaries are at: (1) $^{\text{Y+Z}}(\text{V}_5\text{Cr}_2)$,
308 corresponding to $\text{Na}^{\text{Y}}(\text{V}_3)^{\text{Z}}(\text{V}_2\text{Cr}_2\text{Mg}_2)\text{Si}_6\text{O}_{18}(\text{BO}_3)_3(\text{OH})_3\text{O}$; (2) $^{\text{Y+Z}}(\text{V}_{1.5}\text{Cr}_{5.5})$, corresponding
309 to $\text{Na}^{\text{Y}}(\text{V}_{1.5}\text{Cr}_{1.5})^{\text{Z}}(\text{Cr}_4\text{Mg}_2)\text{Si}_6\text{O}_{18}(\text{BO}_3)_3(\text{OH})_3\text{O}$. Consequently, and assuming that V^{3+} and
310 Cr^{3+} are completely ordered, oxy-chromium-dravite is characterized by V^{3+} contents less than
311 1.5 apfu, vanadio-oxy-chromium-dravite is characterized by V^{3+} contents between 5 and 1.5
312 apfu, and oxy-vanadium-dravite is characterized by V^{3+} contents larger than 5 apfu.

313 With regard to the relations among Al, Cr^{3+} , and V^{3+} in oxy-tourmalines, the current
314 chemical data support complete solid-solution involving V^{3+} , Cr^{3+} and Al (Reznitsky et al.
315 2001; Bosi et al. 2004, 2013a,b).

316

317

318 ACKNOWLEDGMENTS

319 Chemical analyses were carried out with the kind assistance of M. Serracino to whom
320 the authors express their gratitude. L. Reznitskii was supported by a grant from Russian
321 Foundation for Basic Research (project 13-05-00258). We thank F. Colombo and G.R.
322 Rossman for their useful suggestions that improved the manuscript.

323

324

325

REFERENCES CITED

- 326 Agrosi, G., Bosi, F., Lucchesi, S., Melchiorre, G., and Scandale, E. (2006) Mn-tourmaline
327 crystals from island of Elba (Italy): Growth history and growth marks. American
328 Mineralogist, 91, 944-952.
- 329 Bačík, P., Uher, P., Ertl, A., Jonsson, E., Nysten, P., Kanický, V., and Vaculovič, T. (2012)
330 Zoned REE Enriched Dravite from a Granitic Pegmatite in Forshammar Bergslagen
331 Province, Sweden an EPMA, XRD and LA-ICP-MS Study. Canadian Mineralogist. 50,
332 825-841.
- 333 Bosi, F. (2008) Disorder of Fe^{2+} over octahedrally coordinated sites of tourmaline.
334 American Mineralogist, 93, 1647-1653.
- 335 Bosi, F. (2010) Octahedrally coordinated vacancies in tourmaline: a theoretical approach.
336 Mineralogical Magazine, 74, 1037-1044.
- 337 Bosi, F. (2011) Stereochemical constraints in tourmaline: from a short-range to a long-range
338 structure. Canadian Mineralogist, 49, 17-27.
- 339 Bosi, F. (2013) Bond-valence constraints around the O1 site of tourmaline. Mineralogical
340 Magazine, 77, 343-351.
- 341 Bosi, F. and Lucchesi, S. (2004) Crystal chemistry of the schorl-dravite series. European
342 Journal of Mineralogy, 16, 335-344.
- 343 Bosi, F. and Lucchesi, S. (2007) Crystal chemical relationships in the tourmaline group:
344 structural constraints on chemical variability. American Mineralogist, 92, 1054-1063.
- 345 Bosi, F. and Skogby, H. (2013) Oxy-dravite, $\text{Na}(\text{Al}_2\text{Mg})(\text{Al}_5\text{Mg})(\text{Si}_6\text{O}_{18})(\text{BO}_3)_3(\text{OH})_3\text{O}$, a new
346 mineral species of the tourmaline supergroup. American Mineralogist, 98,
347 dx.doi.org/10.2138/am.2013.4441.
- 348 Bosi F., Lucchesi, S., and Reznitskii, L. (2004) Crystal chemistry of the dravite-chromdravite
349 series. European Journal of Mineralogy, 16, 345-352.
- 350 Bosi, F., Balić-Žunić, T., and Surour, A.A., (2010) Crystal structure analysis of four
351 tourmalines from the Cleopatra's Mines (Egypt) and Jabal Zalm (Saudi Arabia), and the
352 role of Al in the tourmaline group. American Mineralogist, 95, 510-518.
- 353 Bosi, F., Reznitskii, L., and Skogby, H. (2012a) Oxy-chromium-dravite,
354 $\text{NaCr}_3(\text{Cr}_4\text{Mg}_2)(\text{Si}_6\text{O}_{18})(\text{BO}_3)_3(\text{OH})_3\text{O}$, a new mineral species of the tourmaline
355 supergroup. American Mineralogist, 97, 2024-2030.
- 356 Bosi, F., Skogby, H., Agrosi, G., and Scandale, E. (2012b) Tsilaisite,
357 $\text{NaMn}_3\text{Al}_6(\text{Si}_6\text{O}_{18})(\text{BO}_3)_3(\text{OH})_3\text{OH}$, a new mineral species of the tourmaline supergroup

- 358 from Grotta d'Oggi, San Pietro in Campo, island of Elba, Italy. *American Mineralogist*,
359 97, 989-994.
- 360 Bosi, F., Reznitskii, L., and Sklyarov, E.V. (2013a) Oxy-vanadium-dravite,
361 $\text{NaV}_3(\text{V}_4\text{Mg}_2)(\text{Si}_6\text{O}_{18})(\text{BO}_3)_3(\text{OH})_3\text{O}$: crystal structure and redefinition of the
362 "vanadium-dravite" tourmaline. *American Mineralogist*. 98, 501-505.
- 363 Bosi, F., Skogby, H., Hålenius, U., and Reznitskii, L. (2013b) Crystallographic and
364 spectroscopic characterization of Fe-bearing chromo-alumino-povondraite and its
365 relations with oxy-chromium-dravite and oxy-dravite. *American Mineralogist*, 98,
366 dx.doi.org/10.2138/am.2013.4447.
- 367 Brown, I.D. and Altermatt, D. (1985) Bond-valence parameters obtained from a systematic
368 analysis of the Inorganic Crystal Structure Database. *Acta Crystallographica*, B41, 244–
369 247.
- 370 Ertl, A., Rossman, G.R., Hughes, J.M., Ma, C., and Brandstätter, F. (2008) V^{3+} -bearing, Mg-
371 rich, strongly disordered olenite from a graphite deposit near Amstall, Lower Austria: A
372 structural, chemical and spectroscopic investigation. *Neues Jahrbuch für Mineralogie*
373 *Abhandlungen*, 184, 243-253.
- 374 Filip, J., Bosi, F., Novák, M., Skogby, H., Tuček, J., Čuda, J., and Wildner, M. (2012) Redox
375 processes of iron in the tourmaline structure: example of the high-temperature treatment
376 of Fe^{3+} -rich schorl. *Geochimica et Cosmochimica Acta*, 86, 239-256.
- 377 Foit, F.F. Jr. (1989) Crystal chemistry of alkali-deficient schorl and tourmaline structural
378 relationships. *American Mineralogist*, 74, 422-431.
- 379 Gonzalez-Carreño, T., Fernandez, M., and Sanz, J. (1988) Infrared and electron microprobe
380 analysis in tourmalines. *Physics and Chemistry of Minerals*, 15, 452-460.
- 381 Grice, J.D. and Ercit, T.S. (1993) Ordering of Fe and Mg in the tourmaline crystal structure:
382 the correct formula. *Neues Jahrbuch für Mineralogie, Abhandlungen*, 165, 245-266.
- 383 Hawthorne, F.C. (1996) Structural mechanisms for light-element variations in tourmaline.
384 *Canadian Mineralogist*, 34, 123-132.
- 385 Hawthorne, F. C. (2002) Bond-valence constraints on the chemical composition of tourmaline.
386 *Canadian Mineralogist*, 40, 789-797.
- 387 Hawthorne, F.C. and Henry, D. (1999) Classification of the minerals of the tourmaline group.
388 *European Journal of Mineralogy*, 11, 201-215.

- 389 Henry, D.J. and Dutrow, B.L. (2011) The incorporation of fluorine in tourmaline: Internal
390 crystallographic controls or external environmental influences? *Canadian Mineralogist*,
391 49, 41-56.
- 392 Henry, D.J., Novák, M., Hawthorne, F.C., Ertl, A., Dutrow, B., Uher, P., and Pezzotta, F.
393 (2011) Nomenclature of the tourmaline supergroup minerals. *American Mineralogist*, 96,
394 895-913.
- 395 Lussier, A.J., Aguiar, P.M., Michaelis, V.K., Kroeker, S., Herwig, S., Abdu, Y., and
396 Hawthorne, F.C. (2008) Mushroom elbaite from the Kat Chay mine, Momeik, near
397 Mogok, Myanmar: I. Crystal chemistry by SREF, EMPA, MAS NMR and Mössbauer
398 spectroscopy. *Mineralogical Magazine*, 72, 747-761.
- 399 Lussier, A.J., Hawthorne, F.C., Aguiar, P.M., Michaelis, V.K., and Kroeker, S. (2011a)
400 Elbaite-liddicoatite from Black Rapids glacier, Alaska. *Periodico di Mineralogia*, 80, 57-
401 73.
- 402 Lussier, A.J., Abdu, Y. Hawthorne, F.C., Michaelis, V.K., Aguiar, P.M., and Kroeker, S.
403 (2011b) Oscillatory zoned liddicoatite from Anjanabonoina, central Madagascar. I.
404 Crystal chemistry and structure by SREF and ^{11}B and ^{27}Al MAS NMR spectroscopy.
405 *Canadian Mineralogist*, 49, 63-88.
- 406 Novák, M., Povondra, P., and Selway, J.B. (2004) Schorl-oxy-schorl to dravite-oxy-dravite
407 tourmaline from granitic pegmatites; examples from the Moldanubicum, Czech
408 Republic. *European Journal of Mineralogy*, 16, 323-333.
- 409 Novák M., Škoda P., Filip J., Macek I., and Vaculovič T. (2011) Compositional trends in
410 tourmaline from intragranitic NYF pegmatites of the Třebíč Pluton, Czech Republic;
411 electron microprobe, Mössbauer and LA-ICP-MS study. *Canadian Mineralogist*, 49,
412 359-380.
- 413 Reznitsky, L.Z., Sklyarov, E.V., Ushchapovskaya, Z.V., Nartova, N.V., Kashaev, A.A.,
414 Karmanov, N.S., Kanakin, S.V., Smolin, A.S., and Nekrosova, E.A. (2001)
415 Vanadiumdravite, $\text{NaMg}_3\text{V}_6[\text{Si}_6\text{O}_{18}][\text{BO}_3]_3(\text{OH})_4$, a new mineral of the tourmaline
416 group. *Zapiski Vsesoyuznogo Mineralogicheskogo Obshchestva*, 130, 59-72 (in
417 Russian).
- 418 Sheldrick, G.M. (2008) A short history of SHELX. *Acta Crystallographica*, A64, 112-122.
- 419 Skogby, H., Bosi, F., and Lazor, P. (2012) Short-range order in tourmaline: a vibrational
420 spectroscopic approach to elbaite. *Physics and Chemistry of Minerals*, 39, 811-816.

- 421 Taran, M.N., Lebedev, A.S., and Platonov, A.N. (1993) Optical absorption spectroscopy of
422 synthetic tourmalines. *Physics and Chemistry of Minerals*, 20, 209-220.
- 423 van Hinsberg, V.J. and Schumacher, J.C. (2011) Tourmaline as a petrogenetic indicator
424 mineral in the Haut-Allier metamorphic suite, Massif Central, France. *Canadian*
425 *Mineralogist*, 49, 177-194.
- 426 van Hinsberg, V.J., Henry, D.J., and Marschall, H.R. (2011) Tourmaline: an ideal indicator of
427 its host environment. *Canadian Mineralogist*, 49, 1-16.
- 428 Wright, S.E., Foley, J.A., and Hughes, J.M. (2000) Optimization of site occupancies in
429 minerals using quadratic programming. *American Mineralogist*, 85, 524-531.
- 430

431

432

LIST OF TABLES

433 **TABLE 1.** Crystal data and details of the single crystal X-ray data collection and refinement for
434 vanadio-oxy-chromium-dravite.

435 **TABLE 2.** Fractional atom coordinates and site occupancy for vanadio-oxy-chromium-dravite.

436 **TABLE 3.** Displacement parameters (\AA^2) for vanadio-oxy-chromium-dravite.

437 **TABLE 4.** Selected bond distances (\AA) for vanadio-oxy-chromium-dravite.

438 **TABLE 5.** X-ray powder diffraction data for vanadio-oxy-chromium-dravite (sample PR76).

439 **TABLE 6.** Chemical composition of vanadio-oxy-chromium-dravite.

440 **TABLE 7.** Cation site populations (atoms per formula unit, apfu), mean atomic number and
441 mean bond distances (\AA) for vanadio-oxy-chromium-dravite.

442 **TABLE 8.** Bond valence calculations (valence unit) for vanadio-oxy-chromium-dravite.

443 **TABLE 9.** Comparative data for oxy-chromium-dravite, vanadio-oxy-chromium-dravite and
444 oxy-vanadium-dravite.

445

446

447

LIST OF FIGURES AND FIGURE CAPTIONS

448 **FIGURE 1.** Polarized FTIR absorption spectra in the (OH)-stretching region of vanadio-oxy-
449 chromium-dravite (sample PR76), vertically offset for clarity. Sample thickness 34
450 μm . The main band around 3535 cm^{-1} is truncated for the *c* direction due to
451 excessive absorption intensity. Spectral ranges where bands related to (OH) in the
452 O1- and O3-sites are expected are indicated.

453 **FIGURE 2.** Polarized electronic spectra for vanadio-oxy-chromium-dravite (sample PR76).
454 Sample thickness $25\ \mu\text{m}$. The inset in the lower left corner shows in detail the
455 spectral range where sharp spin-forbidden Cr^{3+} -bands are characteristic features in
456 spectra of Cr-dominant tourmaline.

457 **FIGURE 3.** Ternary diagram in terms of Al-V-Cr at (*Y* + *Z*) sites for oxy-tourmalines. Black
458 circles: present samples. White circles: sample T89102, oxy-chromium-dravite
459 (Bosi et al. 2012a); and sample N825, oxy-vanadium-dravite (Bosi et al. 2013a).
460 Note that (Al + V + Cr) at the (*Y*+*Z*) sites can add up only to 7 apfu, the remaining
461 two apfu being Mg.

Table 1. Single-crystal X-ray diffraction data details for vanadio-oxy-chromium-dravite

| Sample | PR76 | PR1973 |
|--|---|--|
| Crystal size (mm) | 0.10 × 0.12 × 0.18 | 0.14 × 0.15 × 0.18 |
| <i>a</i> (Å) | 16.1260(2) | 16.1307(5) |
| <i>c</i> (Å) | 7.3759(1) | 7.3792(2) |
| <i>V</i> (Å ³) | 1661.11(4) | 1662.82(9) |
| Range for data collection, 2θ (°) | 5 - 78 | 5 - 73 |
| Reciprocal space range <i>hkl</i> | -24 ≤ <i>h</i> ≤ 24 -28 ≤ <i>k</i> ≤ 27 -12 ≤ <i>l</i> ≤ 12 | -26 ≤ <i>h</i> ≤ 26 -26 ≤ <i>k</i> ≤ 26 -8 ≤ <i>l</i> ≤ 12 |
| Total number of frames | 2543 | 3681 |
| Set of measured reflections | 8934 | 13850 |
| Unique reflections, <i>R</i> _{int} (%) | 2135, 1.50 | 1769, 1.55 |
| Redundancy | 8 | 14 |
| Absorption correction method | SADABS | SADABS |
| Refinement method | Full-matrix last-squares on <i>F</i> ² | Full-matrix last-squares on <i>F</i> ² |
| Structural refinement program | SHELXL-97 | SHELXL-97 |
| Extinction coefficient | 0.00002(7) | 0.00043(7) |
| Flack parameter | 0.05(1) | 0.019(9) |
| <i>wR</i> ₂ (%) | 3.08 | 2.85 |
| <i>R</i> ₁ (%) all data | 1.16 | 1.15 |
| <i>R</i> ₁ (%) for <i>I</i> > 2σ(<i>I</i>) | 1.13 | 1.14 |
| GooF | 1.094 | 1.057 |
| Largest diff. peak and hole (±e ⁻ /Å ³) | 0.28 and -0.28 | 0.45 and -0.37 |

Notes: *R*_{int} = merging residual value; *R*₁ = discrepancy index, calculated from *F*-data; *wR*₂ = weighted discrepancy index, calculated from *F*²-data; GooF = goodness of fit; Diff. Peaks = maximum and minimum residual electron density. Radiation, MoKα = 0.71073 Å. Data collection temperature = 293 K. Space group *R*3*m*; *Z* = 3.

TABLE 2. Fractional atom coordinates and site occupancy for vanadio-oxy-chromium-dravite.

| Sample | PR76 | | | | PR1973 | | | |
|--------|--------------|--------------|-------------|---|--------------|--------------|-------------|---|
| Site | x | y | z | Site occupancy | x | y | z | Site occupancy |
| X | 0 | 0 | 0.22494(15) | Na _{1.002(6)} | 0 | 0 | 0.22692(17) | Na _{0.993(6)} |
| Y | 0.123130(14) | 0.061565(7) | 0.63864(4) | V _{0.974(2)} | 0.123155(12) | 0.061578(6) | 0.63896(4) | V _{1.00} |
| Z | 0.298154(12) | 0.261863(13) | 0.60991(4) | Cr _{0.436(2)} Mg _{0.564(2)} | 0.297932(11) | 0.261752(11) | 0.60924(4) | Cr _{0.510(2)} Mg _{0.490(2)} |
| B | 0.10977(5) | 0.21953(9) | 0.45462(16) | B _{1.00} | 0.10942(4) | 0.21884(9) | 0.4548(2) | B _{1.00} |
| T | 0.189705(15) | 0.188037(15) | 0 | Si _{1.00} | 0.189452(14) | 0.187791(15) | 0 | Si _{1.00} |
| O1 | 0 | 0 | 0.76569(18) | O _{1.00} | 0 | 0 | 0.7652(2) | O _{1.00} |
| O2 | 0.06061(3) | 0.12122(6) | 0.48951(12) | O _{1.00} | 0.06032(3) | 0.12064(6) | 0.49075(14) | O _{1.00} |
| O3 | 0.25651(7) | 0.12825(3) | 0.50956(12) | O _{1.00} | 0.25529(6) | 0.12764(3) | 0.50895(15) | O _{1.00} |
| O4 | 0.09232(3) | 0.18464(7) | 0.07058(12) | O _{1.00} | 0.09231(3) | 0.18461(7) | 0.07087(15) | O _{1.00} |
| O5 | 0.18250(7) | 0.09125(3) | 0.08897(11) | O _{1.00} | 0.18224(6) | 0.09112(3) | 0.08972(13) | O _{1.00} |
| O6 | 0.19178(4) | 0.18257(4) | 0.78153(8) | O _{1.00} | 0.19107(4) | 0.18184(4) | 0.78175(10) | O _{1.00} |
| O7 | 0.28213(4) | 0.28199(4) | 0.07413(8) | O _{1.00} | 0.28211(4) | 0.28189(4) | 0.07298(10) | O _{1.00} |
| O8 | 0.20690(4) | 0.26768(5) | 0.43845(9) | O _{1.00} | 0.20637(4) | 0.26689(4) | 0.43761(11) | O _{1.00} |
| H3 | 0.2676(14) | 0.1338(7) | 0.396(2) | H _{1.00} | 0.2606(14) | 0.1303(7) | 0.393(3) | H _{1.00} |

TABLE 3. Displacement parameters (\AA^2) for vanadio-oxy-chromium-dravite

| Site | U^{11} | U^{22} | U^{33} | U^{23} | U^{13} | U^{12} | $U_{\text{eq}}/U_{\text{iso}}^*$ |
|------|--------------------|------------|-------------|--------------|--------------|-------------|----------------------------------|
| | Sample PR76 | | | | | | |
| X | 0.0215(4) | 0.0215(4) | 0.0200(5) | 0 | 0 | 0.0107(2) | 0.0210(3) |
| Y | 0.00567(8) | 0.00550(7) | 0.00806(7) | -0.00037(3) | -0.00075(5) | 0.00283(4) | 0.00639(5) |
| Z | 0.00432(8) | 0.00477(8) | 0.00596(7) | 0.00044(5) | 0.00004(5) | 0.00218(6) | 0.00506(5) |
| B | 0.0063(3) | 0.0076(5) | 0.0087(4) | 0.0013(3) | 0.00065(17) | 0.0038(2) | 0.00739(19) |
| T | 0.00488(9) | 0.00441(9) | 0.00684(8) | -0.00051(6) | -0.00037(7) | 0.00229(7) | 0.00539(5) |
| O1 | 0.0072(3) | 0.0072(3) | 0.0084(5) | 0 | 0 | 0.00361(17) | 0.0076(2) |
| O2 | 0.0065(2) | 0.0047(3) | 0.0094(3) | 0.0011(2) | 0.00054(12) | 0.00233(16) | 0.00707(14) |
| O3 | 0.0114(4) | 0.0114(3) | 0.0072(3) | 0.00050(13) | 0.0010(3) | 0.00570(19) | 0.01002(15) |
| O4 | 0.0075(2) | 0.0153(4) | 0.0097(3) | -0.0010(3) | -0.00051(14) | 0.0076(2) | 0.00995(15) |
| O5 | 0.0146(4) | 0.0068(2) | 0.0093(3) | 0.00060(14) | 0.0012(3) | 0.0073(2) | 0.00936(15) |
| O6 | 0.0091(2) | 0.0072(2) | 0.0063(2) | -0.00079(17) | -0.00057(17) | 0.0042(2) | 0.00752(10) |
| O7 | 0.0070(2) | 0.0059(2) | 0.0100(2) | -0.00154(17) | -0.00212(18) | 0.00074(19) | 0.00872(10) |
| O8 | 0.0046(2) | 0.0088(3) | 0.0172(2) | 0.00360(19) | 0.00141(19) | 0.0028(2) | 0.01042(11) |
| H3 | | | | | | | 0.015* |
| | Sample 1973 | | | | | | |
| X | 0.0248(4) | 0.0248(4) | 0.0193(7) | 0 | 0 | 0.0124(2) | 0.0229(4) |
| Y | 0.00595(7) | 0.00574(5) | 0.00687(10) | -0.00027(3) | -0.00053(6) | 0.00297(4) | 0.00616(4) |
| Z | 0.00489(7) | 0.00518(7) | 0.00501(9) | 0.00039(5) | 0.00006(5) | 0.00243(5) | 0.00506(5) |
| B | 0.0069(3) | 0.0076(4) | 0.0070(6) | 0.0013(4) | 0.00065(18) | 0.0038(2) | 0.0071(2) |
| T | 0.00559(8) | 0.00528(8) | 0.00577(12) | -0.00057(7) | -0.00039(7) | 0.00267(6) | 0.00556(5) |
| O1 | 0.0070(3) | 0.0070(3) | 0.0076(8) | 0 | 0 | 0.00348(16) | 0.0072(2) |
| O2 | 0.0067(2) | 0.0053(3) | 0.0072(5) | 0.0012(3) | 0.00059(13) | 0.00267(14) | 0.00655(15) |
| O3 | 0.0113(3) | 0.0107(2) | 0.0053(4) | 0.00027(14) | 0.0005(3) | 0.00563(17) | 0.00904(15) |
| O4 | 0.0082(2) | 0.0160(4) | 0.0080(4) | -0.0005(3) | -0.00027(16) | 0.00799(19) | 0.00983(15) |
| O5 | 0.0157(4) | 0.0074(2) | 0.0078(5) | 0.00057(16) | 0.0011(3) | 0.00787(18) | 0.00940(16) |
| O6 | 0.0094(2) | 0.0070(2) | 0.0055(3) | -0.00045(19) | -0.00002(19) | 0.00380(18) | 0.00743(11) |
| O7 | 0.0073(2) | 0.0067(2) | 0.0087(3) | -0.00170(19) | -0.0016(2) | 0.00100(17) | 0.00866(11) |
| O8 | 0.0055(2) | 0.0096(2) | 0.0141(3) | 0.0039(2) | 0.0013(2) | 0.00339(19) | 0.00987(12) |
| H3 | | | | | | | 0.014* |

Notes: Equivalent (U_{eq}) and isotropic (U_{iso}) displacement parameters; H-atom was constrained to have a U_{iso} 1.5 times the U_{eq} value of the O3 oxygen.

Table 4. Selected bond distances (Å) for vanadio-oxy-chromium-dravite

| Sample | PR76 | PR1973 |
|---------------------------|------------|------------|
| X-O2 ^{B,F} (× 3) | 2.5834(12) | 2.5749(14) |
| X-O5 ^{B,F} (× 3) | 2.7389(10) | 2.7398(10) |
| X-O4 ^{B,F} (× 3) | 2.8187(10) | 2.8243(11) |
| <X-O> | 2.714 | 2.713 |
| Y-O1 | 1.9583(7) | 1.9565(8) |
| Y-O6 ^C (× 2) | 1.9960(6) | 1.9871(7) |
| Y-O2 ^B (× 2) | 2.0302(5) | 2.0240(6) |
| Y-O3 | 2.0919(9) | 2.0803(9) |
| <Y-O> | 2.017 | 2.010 |
| Z-O8 ^E | 1.9542(6) | 1.9650(6) |
| Z-O7 ^E | 1.9746(6) | 1.9808(7) |
| Z-O8 | 1.9779(6) | 1.9786(7) |
| Z-O6 | 1.9966(6) | 2.0078(7) |
| Z-O7 ^D | 2.0116(6) | 2.0120(6) |
| Z-O3 | 2.0480(4) | 2.0524(5) |
| <Z-O> | 1.994 | 1.999 |
| B-O8 ^A (× 2) | 1.3617(9) | 1.3603(9) |
| B-O2 | 1.3969(16) | 1.3972(15) |
| <B-O> | 1.373 | 1.373 |
| T-O7 | 1.5992(6) | 1.5998(6) |
| T*-O6 | 1.6151(6) | 1.6144(8) |
| T-O4 | 1.6292(3) | 1.6283(4) |
| T-O5 | 1.6428(4) | 1.6438(4) |
| <T-O> | 1.622 | 1.622 |
| H3-O3 | 0.855(18) | 0.86(2) |

Notes: Standard uncertainty in parentheses. Superscript letters: A = (y - x, y, z); B = (y - x, -x, z); C = (x, x - y, z); D = (y - x + 1/3, -x + 2/3, z + 2/3); E = (-y + 2/3, x - y + 1/3, z + 1/3); F = (-y, x - y, z). Transformations relate coordinates to those of Table 2.

* Positioned in adjacent unit cell.

TABLE 5. X-ray powder diffraction data for vanadio-oxy-chromium-dravite (sample PR76)

| $I_{(meas)}$ (%) | $d_{(meas)}$ (Å) | $d_{(cal)}$ (Å) | h | k | l |
|------------------|------------------|-----------------|-----|-----|-----|
| 100 | 6.509 | 6.519 | 1 | 0 | 1 |
| 19 | 5.060 | 5.067 | 0 | 2 | 1 |
| 19 | 4.629 | 4.650 | 3 | 0 | 0 |
| 31 | 4.293 | 4.289 | 2 | 1 | 1 |
| 40 | 4.022 | 4.027 | 2 | 2 | 0 |
| 53 | 3.564 | 3.564 | 0 | 1 | 2 |
| 47 | 3.022 | 3.021 | 1 | 2 | 2 |
| 42 | 2.611 | 2.610 | 0 | 5 | 1 |
| 19 | 2.225 | 2.225 | 5 | 0 | 2 |
| 42 | 2.171 | 2.173 | 0 | 3 | 3 |
| 40 | 2.075 | 2.072 | 1 | 5 | 2 |
| 27 | 1.948 | 1.947 | 3 | 4 | 2 |
| 16 | 1.688 | 1.689 | 0 | 6 | 3 |
| 16 | 1.538 | 1.538 | 0 | 5 | 4 |

Notes: $I_{(meas)}$ = measured intensity, $d_{(meas)}$ = measured interplanar spacing; $d_{(calc)}$ = calculated interplanar spacing; hkl = reflection indices. Estimated errors in $d_{(meas)}$ -spacing range from 0.02 Å for large d -values to 0.003 Å for small d -values.

TABLE 6. Chemical composition of vanadio-oxy-chromium-dravite

| Sample | PR76 | PR1973 |
|--|-----------|-----------|
| SiO ₂ wt% | 32.75(20) | 32.27(12) |
| TiO ₂ | bdl | 0.07(1) |
| B ₂ O ₃ | 9.56* | 9.40* |
| Al ₂ O ₃ | 7.64(21) | 4.54(19) |
| Cr ₂ O ₃ | 12.87(37) | 24.32(41) |
| V ₂ O ₃ | 24.36(35) | 14.88(27) |
| Fe ₂ O ₃ | 0.42(10)† | 0.86(5)† |
| MgO | 7.19(24) | 7.75(11) |
| ZnO | bdl | 0.10(5) |
| CaO | bdl | 0.05(1) |
| Na ₂ O | 2.52(6) | 2.71(3) |
| K ₂ O | 0.24(3) | 0.08(1) |
| F | 0.25(10) | 0.49(14) |
| H ₂ O | 2.40* | 2.33* |
| -O ≡ F | -0.11 | -0.21 |
| Total | 100.10 | 99.63 |
| Atomic proportions normalized to 31 anions | | |
| Si apfu | 5.95(4) | 5.97(3) |
| Ti ⁴⁺ | - | 0.010(2) |
| B | 3.00 | 3.00 |
| Al | 1.64(4) | 0.99(4) |
| Cr ³⁺ | 1.85(5) | 3.56(5) |
| V ³⁺ | 3.55(5) | 2.21(4) |
| Fe ³⁺ | 0.06(2) | 0.12(1) |
| Mg | 1.95(6) | 2.14(3) |
| Zn | - | 0.014(7) |
| Ca | - | 0.010(3) |
| Na | 0.89(2) | 0.97(1) |
| K | 0.06(1) | 0.018(2) |
| F | 0.14(6) | 0.29(8) |
| OH | 2.91 | 2.87 |

* Calculated by stoichiometry.

† Calculated as Fe³⁺ (see text).

Notes: Errors for oxides are standard deviations (in brackets) of 10 spot analyses. Standard errors for the atomic proportions (in brackets) were calculated by error-propagation theory; bdl = below detection limits; apfu = atoms per formula unit.

TABLE 7. Cation site populations (apfu), mean atomic numbers and mean bond lengths (Å) for vanadio-oxy-chromium-dravite

| Site | Site population | Mean atomic number | | Mean bond length | |
|----------------------|---|--------------------|------------|------------------|-------------|
| | | refined | calculated | refined | calculated* |
| Sample PR76 | | | | | |
| X | 0.89 Na + 0.06 K + 0.05 □ | 11.02(7) | 10.81 | | |
| Y | 2.77 V ³⁺ + 0.17 Mg + 0.06 Fe ³⁺ (2.74 V ³⁺ + 0.24 Mg + 0.02 Fe ³⁺) [†] | 22.40(4) | 22.42 | 2.017 | 2.023 |
| Z | 1.85 Cr ³⁺ + 1.59 Al + 1.78 Mg + 0.78 V ³⁺ (1.82 Cr ³⁺ + 1.65 Al + 1.74 Mg + 0.78 V ³⁺) [†] | 17.24(4) | 17.40 | 1.994 | 1.990 |
| T | 5.95 Si + 0.05 Al | 14 [‡] | 13.99 | 1.622 | 1.621 |
| B | 3 B | 5 [‡] | 5 | | |
| Sample PR1973 | | | | | |
| X | 0.97 Na + 0.02 K + 0.01 □ | 10.93(7) | 11.22 | | |
| Y | 2.21 V ³⁺ + 0.54 Cr ³⁺ + 0.12 Fe ³⁺ + 0.11 Mg + 0.01 Zn + 0.01 Ti ⁴⁺ (2.20 V ³⁺ + 0.57 Cr ³⁺ + 0.12 Fe ³⁺ + 0.10 Mg + 0.02 Zn) [†] | 23 [‡] | 22.97 | 2.010 | 2.014 |
| Z | 3.01 Cr ³⁺ + 2.03 Mg + 0.96 Al (2.98 Cr ³⁺ + 2.04 Mg + 0.98 Al + 0.03 Ti ⁴⁺) [†] | 18.12(4) | 18.19 | 1.999 | 1.997 |
| T | 5.97 Si + 0.03 Al | 14 [‡] | 13.99 | 1.622 | 1.621 |
| B | 3 B | 5 [‡] | 5 | | |

Notes: apfu = atoms per formula unit;

* Calculated using the ionic radii of Bosi and Lucchesi (2007).

[†] Site populations optimized by the procedure of Wright et al. (2000).

[‡] Fixed in the final stages of refinement

Table 8. Bond valence calculations (valence unit) for vanadio-oxy-chromium-dravite.

| Site | X | Y | Z | T | B | Σ |
|---------------|----------------------|-----------------------|----------------------|----------------------|----------------------|------|
| PR76 | | | | | | |
| O1 | | 0.55 ^{x3} → | | | | 1.65 |
| O2 | 0.13 ^{x3} ↓ | 0.46 ^{x2} ↓→ | | | 0.93 | 1.97 |
| O3 | | 0.39 | 0.39 ^{x2} → | | | 1.17 |
| O4 | 0.07 ^{x3} ↓ | | | 0.99 ^{x2} → | | 2.04 |
| O5 | 0.08 ^{x3} ↓ | | | 0.95 ^{x2} → | | 1.99 |
| O6 | | 0.50 ^{x2} ↓ | 0.45 | 1.02 | | 1.97 |
| O7 | | | 0.47 | 1.07 | | 1.97 |
| | | | 0.43 | | | |
| O8 | | | 0.47 | | 1.03 ^{x2} ↓ | 2.00 |
| | | | 0.50 | | | |
| Σ | 0.84 | 2.85 | 2.71 | 4.03 | 2.99 | |
| MFV | 0.94 | 2.92 | 2.70 | 3.99 | 3.00 | |
| PR1973 | | | | | | |
| O1 | | 0.53 ^{x3} → | | | | 1.60 |
| O2 | 0.13 ^{x3} ↓ | 0.46 ^{x2} ↓→ | | | 0.93 | 1.98 |
| O3 | | 0.40 | 0.39 ^{x2} → | | | 1.18 |
| O4 | 0.06 ^{x3} ↓ | | | 0.99 ^{x2} → | | 2.04 |
| O5 | 0.08 ^{x3} ↓ | | | 0.95 ^{x2} → | | 1.98 |
| O6 | | 0.51 ^{x2} ↓ | 0.44 | 1.03 | | 1.97 |
| O7 | | | 0.47 | 1.07 | | 1.97 |
| | | | 0.43 | | | |
| O8 | | | 0.47 | | 1.03 ^{x2} ↓ | 1.99 |
| | | | 0.49 | | | |
| Σ | 0.82 | 2.88 | 2.69 | 4.03 | 2.99 | |
| MFV | 1.01 | 2.96 | 2.66 | 3.99 | 3.00 | |

*MFV = mean formal valence from site populations.

TABLE 9. Comparative data for oxy-chromium-dravite, vanadio-oxy-chromium-dravite and oxy-vanadium-dravite.

| | Oxy-chromium-dravite | Vanadio-oxy-chromium-dravite | Oxy-vanadium-dravite |
|----------------------------|------------------------------------|----------------------------------|--|
| <i>a</i> (Å) | 16.05 -16.11 | 16.13 | 16.19 |
| <i>c</i> | 7.32 -7.37 | 7.38 | 7.41 |
| <i>V</i> (Å ³) | 1634 -1656 | 1662 | 1683 |
| Space group | <i>R3m</i> | <i>R3m</i> | <i>R3m</i> |
| Optic sign | Uniaxial (–) | Uniaxial (–) | Uniaxial (–) |
| ω | 1.765 | 1.767 | 1.786 |
| ϵ | 1.715 | 1.710 | 1.729 |
| Streak | Green | Green | Yellowish-brownish |
| Color | Emerald-green | Green | Dark green to black |
| Pleochroism | O = dark-green E = yellow-green | O = dark green E = pale green | O = dark brownish green E = yellowish green |
| Reference | Bosi et al. (2012a). | This work. | Reznitsky et al. (2001); Bosi et al. (2013a) |

Notes: The range in unit-cell parameters for oxy-chromium-dravite represents data for two different samples (Bosi et al. 2012a)

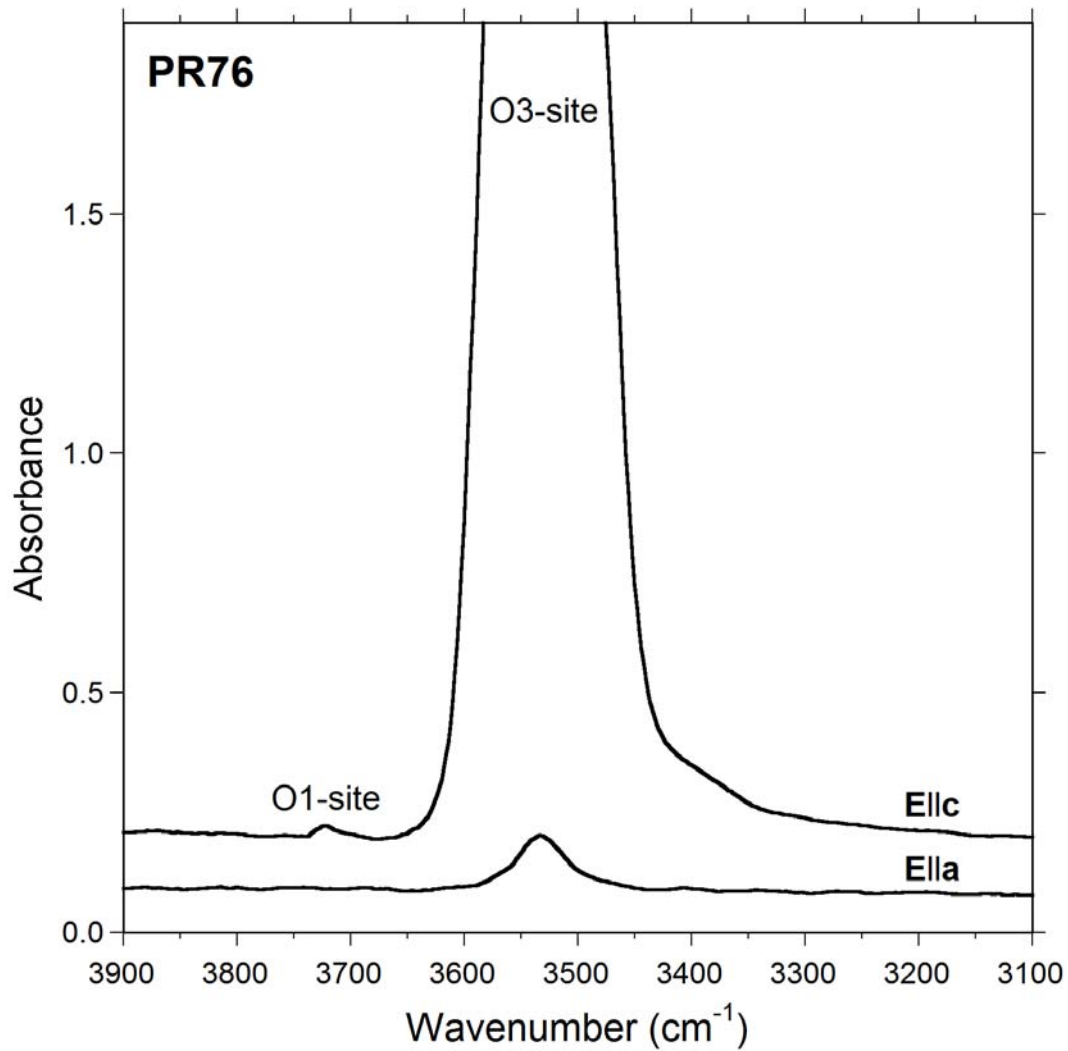


FIGURE 2

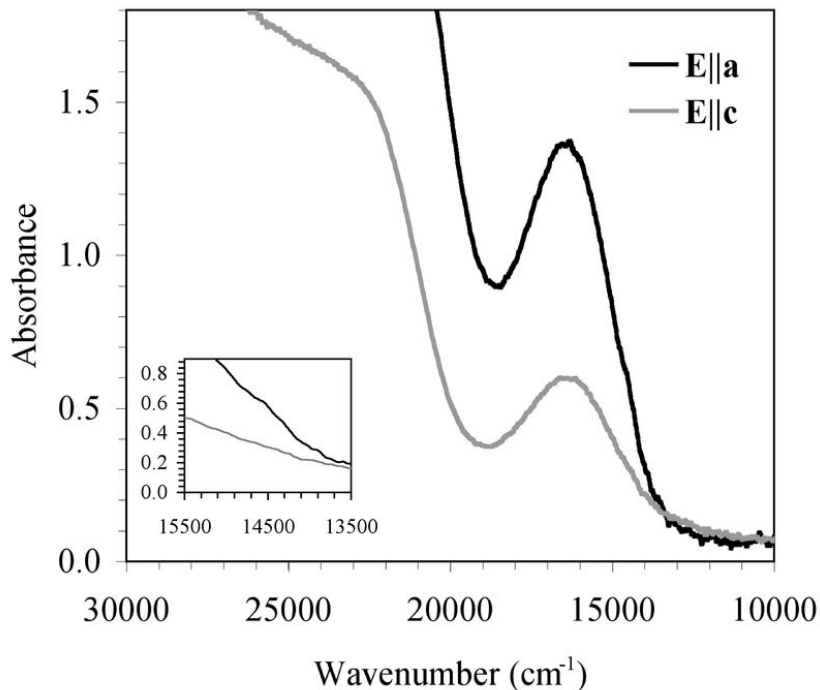


FIGURE 3

